GEOPHYSICS, VOL. 60, NO. 2 (MARCH-APRIL 1995); P. 522-530, 5 FIGS.

Forbidden directions for inhomogeneous pure shear waves in dissipative anisotropic media

José M. Carcione* and Fabio Cavallini*

ABSTRACT

In this work we investigate the wave-propagation properties of pure shear, inhomogeneous, viscoelastic plane waves in the symmetry plane of a monoclinic medium. In terms of seismic propagation, the problem is to describe *SH-waves* traveling through a fractured transversely isotropic formation where we assume that the waves are inhomogeneous with amplitudes varying across surfaces of constant phase. This assumption is widely supported by theoretical and experimental evidence.

The results are presented in terms of polar diagrams of the quality factor, attenuation, slowness, and energy velocity curves. Inhomogeneous waves are more anisotropic and dissipative than homogeneous viscoelastic plane waves, for which the wavenumber and attenuation directions coincide. Moreover, the theory predicts, beyond a given degree of inhomogeneity, the existence of "stop bands" where there is no wave propagation. This phenomenon does not occur in dissipative isotropic and elastic anisotropic media. The combination of anelasticity and anisotropy activates these bands. They exist even in very weakly anisotropic and quasi-elastic materials; only a finite value of Q is required. Weaker anisotropy does not affect the width of the bands, but increases the threshold of inhomogeneity above which they appear; moreover, near the threshold, lower attenuation implies narrower bands. A numerical simulation suggests that, in the absence of material interfaces or heterogeneities, the wavefield is mainly composed of homogeneous waves.

INTRODUCTION

Inhomogeneous anelastic plane waves have the property that the wavenumber and attenuation vectors do not point in the same direction. This implies that equiphase planes (normal to the wavenumber vector, see Figure 1) do not coincide with equiamplitude planes (normal to the attenuation). The theory of propagation of plane inhomogeneous waves in viscoelastic isotropic media has been investigated by several researchers, notably Buchen (1971), Borcherdt (1977), and Krebes (1984). Hosten et al. (1987) compared theoretical and experimental results of inhomogeneous waves generated at a liquid/solid interface where the solid is a low-loss hexagonal medium, and the' equiamplitude planes are parallel to the interface. At anelastic (elastic)-anelastic interfaces separating isotropic media, an *SH*-wave incident at an angle of 30 degrees produces an inhomogeneous transmitted wave with an inhomogeneity angle γ_t of 60 degrees or more, depending on the material properties (Borcherdt et al., 1986). Similarly, Winterstein (1987) shows (e.g., in his Figure 4) that strong contrasts in the quality factor at an interface produce transmitted inhomogeneous waves with an inhomogeneity angle γ_t of nearly 90 degrees for almost all γ_i and propagation directions in the incidence layer. Inhomogeneous waves are also part of interface waves (Carcione, 1992a).

A transversely isotropic formation with an embedded set of inclined parallel fractures can be represented by a monoclinic medium. When the plane of mirror symmetry of this medium is vertical, the pure antiplane strain waves are SE&waves. The fractures induce intrinsic attenuation when they are filled with fluids. The result is that velocity dispersion alters the shape of the wavefront (an ellipse in the elastic case), and that the amplitude of the signal is not isotropic along the wavefront as a result of anisotropic dissipation. For shortness, here and below the term "wavefront" indicates the intersection of the 3-D wavefront with the plane of symmetry. In this work, part of which has already been presented as an expanded abstract (Carcione and Cavallini, 1993c), we consider pure shear-wave propa-

Manuscript received by the Editor October 22, 1993; revised manuscript received August 2, 1994.
*Osservatorio Geofisico Sperimentale, P.O. Box 2011, I-34016 Trieste, Italy.

gation in the mirror symmetry plane of a monoclinic medium. Propagation in this plane is the most general situation for which antiplane strain motion exists at all propagation angles. On the other hand, pure shear-wave propagation in transversely isotropic media is a degenerate case. Our main result is that, beyond a given threshold of inhomogeneity angle, there exist stop bands in the propagation angle. The assumptions in the geological model are not crucial. Indeed, the stop bands are expected also for waves propagating outside planes of symmetry. However, this is the simplest such case (apart from the transversely isotropic, corresponding to $c_{46} = 0$); and, very often, a deep understanding of a phenomenon requires disregarding realistic, but somewhat secondary, details.

DISPERSION RELATION

The stress-strain relation for a linear anisotropic and viscoelastic medium can be expressed as (Carcione and Cavallini, 1993a; Carcione, 1994)

$$\mathbf{T} = \mathbf{p} \cdot \mathbf{S}, \tag{1}$$

where

$$\mathbf{T} \equiv [T_1, T_2, T_3, T_4, T_5, T_6]^{\mathsf{T}} = [\sigma_{xx}, \sigma_{yy}, \sigma_{zz}, \sigma_{yz}, \sigma_{xz}, \sigma_{xy}]^{\mathsf{T}} \tag{2}$$

is the stress vector,

$$\mathbf{S} \equiv [S_1, S_2, S_3, S_4, S_5, S_6]^{\mathsf{T}} = [\varepsilon_{xx}, \varepsilon_{yy}, \varepsilon_{zz}, 2\varepsilon_{yz}, 2\varepsilon_{xz}, 2\varepsilon_{xy}]^{\mathsf{T}} \tag{3}$$

is the strain vector, and $\mathbf{p}$ is the symmetric stiffness matrix whose components are complex and frequency-dependent. The dot denotes ordinary matrix multiplication, and the superscript T indicates the transpose.

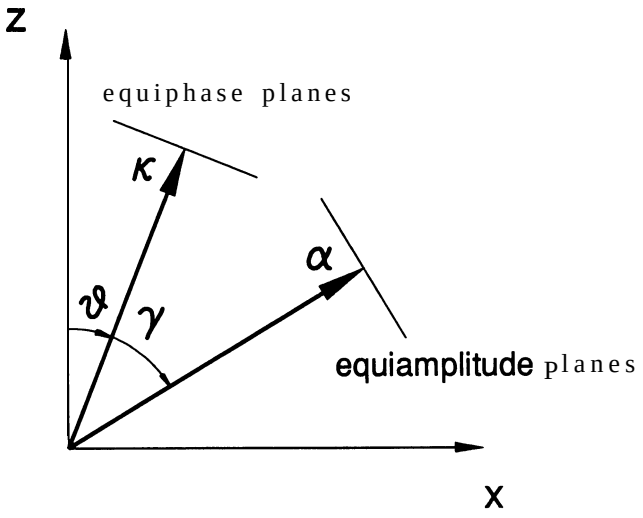

FIG. 1. Wavenumber and attenuation vectors of an inhomogeneous viscoelastic plane wave. The angle θ defines the propagation direction and γ the degree of inhomogeneity of the wave.

A general solution for the displacement field can be represented as a superposition of viscoelastic plane waves of the form

$$\mathbf{u} = \mathbf{U}_0 e^{\iota(\omega t - \mathbf{k} \cdot \mathbf{x})}, \tag{4}$$

where $\iota = \sqrt{-1}$, ω is the angular frequency, and $\mathbf{U}_0$ is a constant complex vector. The wavenumber k is in general complex and can be written as

$$\mathrm{k} = \mathrm{K} - \iota\boldsymbol{\alpha}, \tag{5}$$

where K and $\boldsymbol{\alpha}$ are the real wavenumber and attenuation vectors, indicating the directions and magnitudes of propagation and attenuation, respectively. In general, these directions are different (Figure 1) and the plane wave is termed inhomogeneous. If the directions of propagation and attenuation coincide, the wave is called homogeneous. As we shall see in the next section, an alternative parameterization of the 2-D plane wave is through the magnitude of the propagation and attenuation vectors, and their respective direction angles. When the propagation vector is the plane of mirror symmetry of a monoclinic medium, the global dispersion relation separates into a quadratic factor and a linear factor representing the dispersion relation of the antiplane shear wave with displacement field

$$\mathrm{u} = U_0 \hat{\mathbf{e}}_y e^{\iota(\omega t - k_x x - k_z z)}, \tag{6}$$

where k_x and k_z are complex quantities. That k is in the (x, z)-plane is supported by the fact that any kind of symmetry possessed by the attenuation follows the symmetry of the crystallographic form of the material. These statements are derived from an empirical law known as Neumann's principle (Neumann, 1885). This implies that the symmetries of any property must be higher or equal to the intrinsic symmetries of the solid. The dispersion relation of the viscoelastic shear wave is similar to that of the corresponding elastic wave [*Auld*, 1990], but the stiffnesses and wavenumber components are complex and frequency-dependent, leading to

$$p_{66}k_x^2 + 2p_{46}k_x k_z + p_{44}k_z^2 - \rho\omega^2 = 0, \tag{7}$$

where p is the material density.

SLOWNESS, PHASE VELOCITY, AND ATTENUATION VECTORS

The wavenumber components can be written as

$$k_x = \kappa\ell_x - \iota\alpha m_x \quad \text{and} \quad k_z = \kappa\ell_z - \mathrm{mm}_{,,} \tag{8}$$

where $\hat{\boldsymbol{\kappa}} = (\ell_x, \ell_z)$ and $\hat{\boldsymbol{\alpha}} = (m_{,,}, m_{,})$ are unit vectors defining the propagation and attenuation directions, respectively. As illustrated in Figure 1, they can be expressed in terms of θ and γ as

$$\ell_x = \sin\theta, \qquad \ell_z = \cos\theta, \tag{9}$$

and

$$m_x = \sin(\theta + \gamma), \qquad m_z = \cos(\theta + \gamma), \tag{10}$$

where $\gamma = \arccos(\hat{\boldsymbol{\kappa}}^{\mathsf{T}} \cdot \hat{\boldsymbol{\alpha}})$. We consider here that $-90° \le \gamma \le 90°$, i.e., the amplitude decreases in equiphase planes, although in the dissipative isotropic case $\gamma = \pm 90$ degrees is

forbidden (Buchen, 1971). It is important to note that γ is a free parameter of the theory, in the sense that arbitrary values of γ are possible depending on the incident wave and the material properties of the media.

The problem is now to express the real wavenumber κ and the real attenuation $\boldsymbol{\alpha}$ in terms of the angular frequency ω and the directions $\hat{\boldsymbol{\kappa}}$ and $\hat{\boldsymbol{\alpha}}$. Substituting the wavenumber components [equation (8)] into the dispersion relation (7) and reordering terms gives

$$a\kappa^2 - b\alpha^2 - 2\imath c\kappa\alpha = \omega^2, \tag{11}$$

where

$$\rho a = p_{66}\ell_x^2 + 2p_{46}\ell_x\ell_z + p_{44}\ell_z^2, \tag{12}$$

$$\rho b = p_{66}m_x^2 + 2p_{46}m_x m_z + p_{44}m_z^2, \tag{13}$$

and

$$\rho c = p_{66}\ell_x m_x + p_{46}(\ell_x m_z + \ell_z m_x) + p_{44}\ell_z m_z. \tag{14}$$

The imaginary part of equation (11) yields the following relationship between κ and a:

$$\alpha = q\kappa, \tag{15}$$

where

$$q = a_{\Im}/[c_{\Re} + (c_{\Re}^2 + a_{\Im}b_{\Im})^{1/2}], \tag{16}$$

with the subscripts $\Re$ and 3 denoting real and imaginary parts, respectively. Substituting relation (16) into the real part of equation (11) gives the expression for the real wavenumberi

$$\mathrm{K} = \omega/(a_{\Re} - q^2 b_{\Re} + 2qc_{\Im})^{1/2}. \tag{17}$$

Note that $a_{\Re} - q^2 b_{\Re} + 2qc_{\Im} \equiv V_p^2$ is the square of the phase velocity and must be a positive quantity. Therefore, the real wavenumber and attenuation vectors are

$$\mathrm{K} = \kappa\hat{\boldsymbol{\kappa}}, \tag{18}$$

and

$$\boldsymbol{\alpha} = q\kappa\hat{\boldsymbol{\alpha}}. \tag{19}$$

The slowness vector and the phase velocity are

$$\mathbb{S} = \frac{\mathrm{K}}{\omega}\boldsymbol{\kappa}, \tag{20}$$

and

$$\mathbf{V}_p = \frac{\omega}{\kappa}\boldsymbol{\kappa}, \tag{21}$$

respectively. If $\gamma = 0$, then $\hat{\boldsymbol{\alpha}} = \hat{\boldsymbol{\kappa}}$, and $c = b = a \equiv V^2$, where V is the complex velocity of homogeneous waves introduced in Carcione (1990) and Carcione (1992b) for a transversely isotropic medium, and in Carcione (1994) for an orthorhombic medium.

ENERGY BALANCE EQUATION

The Umov-Poynting theorem, or energy balance equation, for inhomogeneous plane waves in the absence of body forces (Carcione and Cavallini, 1993a) is

$$2\hat{\boldsymbol{\alpha}}^{\mathsf{T}}\,\mathrm{l}\,\mathrm{P} + 2\imath\omega[\langle\varepsilon_s\rangle - \langle\varepsilon_v\rangle] - \omega\langle\varepsilon_d\rangle = 0, \tag{22}$$

where P is the complex Umov-Poynting vector defined as

$$\mathrm{P} = -\tfrac{1}{2}\underline{\boldsymbol{\Sigma}}\cdot\dot{\mathbf{u}}^*, \tag{23}$$

with $\underline{\boldsymbol{\Sigma}}$ the stress tensor given by

$$\underline{\boldsymbol{\Sigma}} = \begin{bmatrix} T_1 & T_6 & T_5 \\ T_6 & T_2 & T_4 \\ T_5 & T_4 & T_3 \end{bmatrix}. \tag{24}$$

The asterisk used as superscript denotes complex conjugation. The real part of the Umov-Poynting vector gives the average power flow density over a cycle. The quantities

$$\langle\varepsilon_s\rangle = \tfrac{1}{4}\Re[\mathbf{S}^{\mathsf{T}}\cdot\mathbf{p}\cdot\mathbf{S}^*] \tag{25}$$

and

$$\langle\varepsilon_v\rangle = \tfrac{1}{4}\rho\dot{\mathbf{u}}^{\mathsf{T}}\cdot\dot{\mathbf{u}}^* \tag{26}$$

are the time average strain and kinetic energy densities, and

$$\langle\varepsilon_d\rangle = \tfrac{1}{2}\Im[\mathbf{S}^{\mathsf{T}}\cdot\underline{\mathbf{p}}\cdot\mathbf{S}^*] \tag{27}$$

is the dissipated energy density, where $\Re[\cdot]$ and $\Im[\cdot]$ take the real and the imaginary part, respectively. The Umov-Poynting vector and energy densities for shear waves in the plane of mirror symmetry of a monoclinic medium are calculated in Appendix A. These quantities are used in the following sections to compute the energy velocity vector and the quality factor.

ENERGY VELOCITY AND WAVEFRONT

The energy velocity is the ratio of the average power flow density $\Re[\mathbf{P}]$ to the mean energy density (E) = $\langle\varepsilon_v + \varepsilon_s\rangle$ Hence

$$\mathbf{V}_e = \frac{\Re[\mathbf{P}]}{\langle\varepsilon_v + \varepsilon_s\rangle}. \tag{28}$$

Substitution of the Umov-Poynting vector (A-5), and the energy densities (A-6) and (A-10) into equation (28) gives the energy velocity for inhomogeneous shear waves:

$$\mathbf{V}_e = \frac{2\Re[(p_{46}k_z + p_{66}k_x)\hat{\mathbf{e}}_x + (p_{44}k_z + p_{46}k_x)\hat{\mathbf{e}}_z]}{\rho\omega(1 + V_p^{-2}\Re[a + q^2 b])}, \tag{29}$$

where equation (21) has been used.

QUALITY FACTOR

Roughly speaking, the quality factor is the ratio of stored energy to dissipated energy. In mathematical terms, two alternative definitions are found in the literature:

$$\mathrm{Q} = \frac{(\varepsilon_s)_{\mathrm{peak}}}{\langle\varepsilon_d\rangle}, \qquad \mathrm{Q}' = \frac{2\langle\varepsilon_s\rangle}{\langle\varepsilon_d\rangle}, \tag{30}$$

where angular brackets indicate time averaging over a cycle. When the plane wave is homogenous, the two definitions are

equivalent, but for inhomogeneous waves they differ. Using the average strain energy, the quality factor reads

$$Q' = \frac{2\langle \varepsilon_s \rangle}{\langle \varepsilon_d \rangle} = \frac{\Re[a + q^2 b]}{\Im[a + q^2 b]}, \tag{31}$$

by virtue of equations (A-10) and (A-11). The calculation of the peak strain energy density for inhomogeneous waves is carried out in Appendix B for a general anisotropic medium. For the antiplane shear wave in a monoclinic medium, it is given by

$$(\varepsilon_s)_{\text{peak}} = (\Re[\mathbf{S}^{\top}] \, \Re[\mathbf{p}] \, \Re[\mathbf{S}])_{\text{peak}} = \langle \varepsilon_s \rangle + \Delta, \tag{32}$$

where

$$\begin{aligned} 16\Delta^2 = {} & |S_4|^4 p_{44\Re}^2 + |S_6|^4 p_{66\Re}^2 + 4|S_4|^2 |S_6|^2 p_{46\Re}^2 \\ & + 2|S_4|^2 |S_6|^2 p_{44\Re} p_{66\Re} \cos[2(\phi_4 - \phi_6)] \\ & + 4|S_4||S_6|(p_{44\Re}|S_4|^2 + p_{66\Re}|S_6|^2) p_{46\Re} \\ & \times \cos(\phi_4 - \phi_6), \end{aligned} \tag{33}$$

with ϕ_4 and ϕ_6 the arguments of S_4 and S_6, respectively. Note that, from equations (A-l) and (A-2), ϕ_4 = -n/2 + arg U_0 + arg k_z − K l X and $\phi_6 = -\pi/2$ + arg U_0 + arg k_x − K l x. Hence, the peak value depends on the phase difference $\phi_4 - \phi_6$ = arg (k_z) − arg (k_x) only. Substituting the strains (A-l) and (A-2) into equation (33) gives

$$\begin{aligned} 16\Delta^2 = {} & |U_0|^4 e^{-4\boldsymbol{\alpha}\cdot\mathbf{x}} \{ |k_z|^4 p_{44\Re}^2 + |k_x|^4 p_{66\Re}^2 \\ & + 4|k_z|^2 |k_x|^2 p_{46\Re}^2 + 2|k_z|^2 |k_x|^2 p_{44\Re} p_{66\Re} \\ & \times \cos[2(\phi_4 - \phi_6)] + 4|k_z||k_x|(p_{44\Re}|k_z|^2 \\ & + p_{66\Re}|k_x|^2) p_{46\Re} \cos(\phi_4 - \phi_6) \}. \end{aligned} \tag{34}$$

The quality factor is then given by

$$Q = \frac{(\varepsilon_s)_{\text{peak}}}{\langle \varepsilon_d \rangle} = \frac{\langle \varepsilon_s \rangle + \Delta}{\langle \varepsilon_d \rangle}. \tag{35}$$

We demonstrate in Appendix B that when the wave is homogeneous, A = $\langle \varepsilon_s \rangle$ and Q = Q'. It can be seen that, if γ = 0, then $\mathbf{V}_e$ and Q reduce to the respective correct expressions for homogeneous waves (Carcione 1992b, 1994). Moreover, it can be shown that K, $\boldsymbol{\alpha}$, $\mathbf{V}_p$, P, $\langle \varepsilon_s \rangle$, $\langle \varepsilon_v \rangle$, and $\langle \varepsilon_d \rangle$ satisfy certain fundamental relations found by Carcione and Cavallini (1993a) for general wave propagation in anisotropic-viscoelastic media.

EXAMPLES

We consider a monoclinic medium with $p_{44} = c_{44} M_1$, $p_{66} = c_{66} M_2$ and $p_{46} = c_{46}$, where

$$M_\nu = \frac{1 + \iota\omega\tau_{\varepsilon\nu}}{1 + \iota\omega\tau_{\sigma\nu}}, \qquad \nu = 1, 2, \tag{36}$$

and where $\tau_{\varepsilon\nu}$ and $\tau_{\sigma\nu}$ are the material relaxation times characterizing the dissipation mechanisms of the shear wave. The quality factors for homogeneous waves (γ = 0) along the z and x axes are

$$Q_\nu(\omega) = Q_{0\nu} \frac{1 + \omega^2 \tau_0^2}{2\omega\tau_0}, \qquad \nu = 1, 2,$$

respectively, where $Q_{0\nu} = 2\tau_0/(\tau_{\varepsilon\nu} - \tau_{\sigma\nu})$ and $\tau_0 = \sqrt{\tau_{\varepsilon\nu}\tau_{\sigma\nu}}$ (Carcione, 1994). The curve Q,,(o) has its peak at $\omega_0 = 1/\tau_0$, and the value of Q_ν at the peak is $Q_{0\nu}$. The values of the low-frequency elasticities are c_{44} = 10.0 GPa, c_{66} = 22.5 GPa, and c_{46} = 5 .O GPa. The relaxation peaks of both dissipation mechanisms are centered at $f_0 = 2\pi/\tau_0$ (the numerical value of τ_0 being immaterial), and the values of the peak quality factors are Q_{01} = 5 and Q_{02} = 10. As mentioned before, they correspond to the quality factors of the homogeneous plane wave along the z- and x-directions, respectively. Figure 2 displays polar diagrams of the quality factor, attenuation, slowness, and energy velocity for an inhomogeneous wave with γ = 60 degrees. The curves correspond to a frequency of f_0, with the broken lines representing the properties of the homogeneous wave. The orientation and shape of the curves depend, first, on the propagation direction, magnitude, and sign of γ, which are characteristics of the wave, and, second, on the elasticities and dissipation mechanisms, which are intrinsic properties of the medium. As can be observed, the inhomogeneous wave is more strongly attenuated than the homogeneous wave. Also, it can be inferred that the curves deviate more strongly from the isotropic shape for increasing values of γ and along certain directions of propagation. This effect is noticeable in the attenuation curve. Figure 3a and 3b represent V_p^2 as a function of θ, the propagation angle, where the broken line corresponds to the homogeneous wave (γ = 0). Figure 3b corresponds to vertical and horizontal quality factors of $Q_{01} = Q_{02}$ = 100. Observe that in the transition from γ = 60 degrees to γ = 68 degrees, two "stops bands" develop (for $\gamma > \gamma_0 \approx 64$ degrees) where the wave does not propagate (Figure 3a). These bands, corresponding to $V_p^2 < 0$, occur exclusively in dissipative anisotropic media; they do not exist in dissipative isotropic or elastic anisotropic materials. Note that the stop bands exist even for high values of Q, as is the case in Figure 3b. The behavior is such that they exist for any finite value of Q, with their width decreasing with increasing Q. This phenomenon is not to be confused with the stop bands considered by, e.g., Silva (1992), since in that case the band is in the frequency domain, and for layered structures.

Our results are somewhat similar to the so-called Rayleigh windows observed by Borcherdt et al. (1986) in anelastic-anelastic interfaces separating isotropic media. In that window, close to the critical angle, the reflection amplitude is reduced considerably. The differences from our problem is that here the medium is anisotropic and there is no material interface. Moreover, propagation is forbidden within the stop bands. For illustration, Figure 4 shows the quality factor and the energy velocity, for γ = 68°. These curves correspond to the material whose properties are represented in Figures 2 and 3a. For this material, other results (not plotted here) are that: (1) the bands also exist for transversely isotropic media (i.e., c_{46} = 0); (2) for higher Q they appear before (lower values of γ) they do for lower Q (although there is a lower limit for γ below which the bands do not exist, see Figure 3b); (3) weaker anisotropy does not imply narrower bands but yields a higher inhomogeneity threshold; (4) for very low and very high frequencies the bands appear in correspondence to lower

values of γ and, for a given γ, the bandwidth is larger for very low frequencies; (5) when $\gamma < 0$ the location and shapes of the bands are symmetric (mirror symmetry) with respect to the principal axes (e.g., a symmetry axis in a transversely isotropic solid), compared to $\gamma > 0$; and (6) when $\gamma = 90$ degrees, each band covers a solid angle of $\pi/2$. The existence of inhomogeneous body waves for $\gamma = 90$" is forbidden in isotropic media (Winterstein, 198'7). Let us consider, for instance, the case $c_{46} = 0$, $\theta = 0$ degrees, and $\gamma = 90°$. It can be readily verified that

$$V_p^2 = (Q_{01} - Q_{02})(p_{44\Im}/\rho),$$
$$\alpha^2 = \frac{\omega^2}{(p_{66\Im}/\rho)}(Q_{01} - Q_{02})^{-1}1 \tag{37}$$

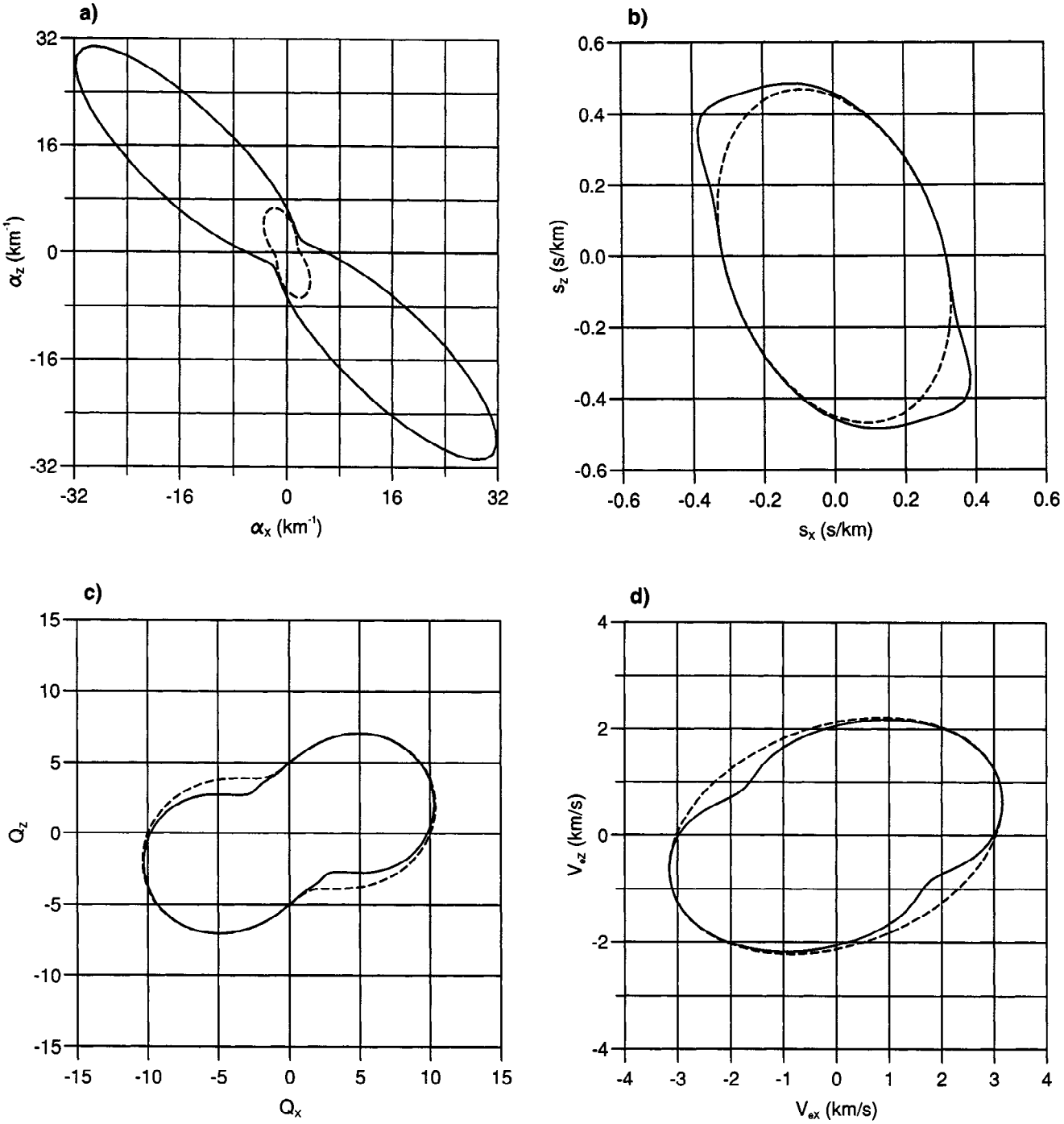

FIG. 2. Polar representations of (a) attenuation, (b) slowness, (c) quality factor, and (d) energy velocity for an inhomogeneous wave (γ = 60 degrees) in the symmetry plane of a monoclinic medium. The curves correspond to a frequency of f_0, where the quality factor takes the minimum value. The broken lines represent the properties of the homogeneous wave (γ = 0). Differences between the homogeneous and inhomogeneous waves are evident along certain directions.

Thus, for $Q_{01} > Q_{02}$ there is propagation and attenuation (it can be easily shown that $p_{663} > 0$). Conversely, for $\theta = 90°$ and $\gamma = 90°$, the wave exists for $Q_{02} > Q_{01}$. In isotropic media ($Q_{01} = Q_{02}$) there is no propagation. A forward modeling code has been developed to simulate anelastic waves in the symmetry plane of a monoclinic medium (Carcione and Cavallini, 1993b). This code is based on the generalized version of the SH-wave equation and uses the rheological relation previously introduced in the time-domain. The results of the simulations are shown in Figure 5 by snapshots of the elastic and anelastic wavefields produced by a line source normal to the symmetry plane of the monoclinic medium. The source is a Ricker wavelet with a central frequency of f_0. The wavefield attenuates more in the vertical direction, as indicated by the quality factor and attenuation curves in Figure 2. Besides the anisotropic attenuation effect, strong velocity dispersion is seen since the anelastic wavefront is larger than the elastic wavefront. From a comparison of the snapshot in Figure 5b with the energy velocity polar plots represented in Figure 26, the wavefield seems mostly a superposition of homogeneous plane waves. This is a result of the fact that the medium is homogeneous. When interfaces or inhomogeneities are present, inhomogeneous waves are the rule, not the exception. These snapshots were successfully tested with an analytical solution found by Carcione and Cavallini (1993d).

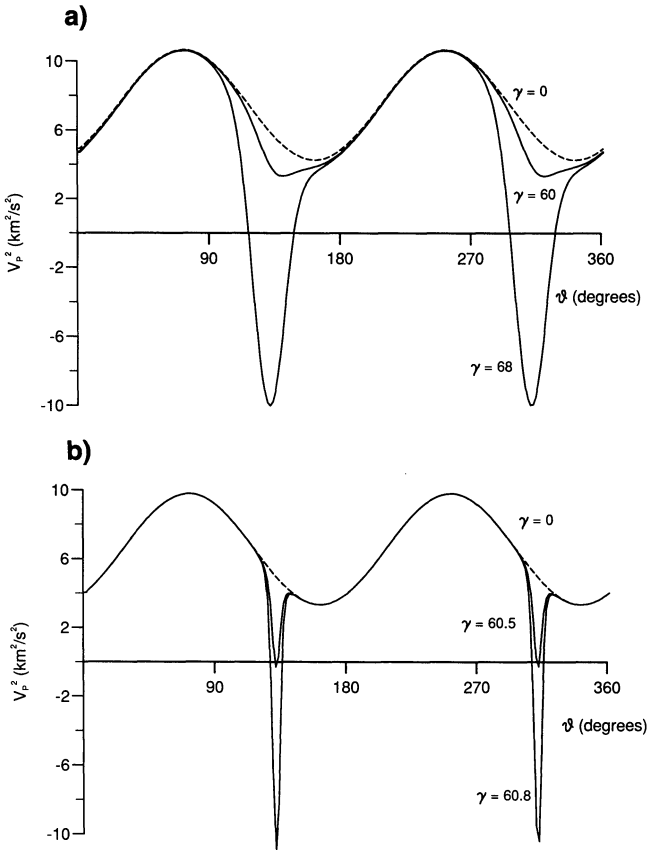

FIG. 3. Square of the phase velocity, V_n^2, as a function of the propagation angle θ for different values of γ. In (a), the medium has vertical and horizontal quality factors of $Q_{01} = 5$ and $Q_{02} = 10$, respectively; and in (b) $Q_{01} = Q_{02} = 100$. Stop bands exist where there is no propagation. For higher values of Q the bands are narrower.

CONCLUSIONS

Increasing values of γ, the angle between the propagation and attenuation directions, increase the dissipation and anisotropy of a medium beyond values calculated for homogeneous waves. In fact, while wavefronts based on the homogeneity assumption may appear isotropic, wavefronts composed of inhomogeneous waves can deviate considerably from a circle. Furthermore, beyond a given inhomogeneity angle, the combined anelastic-anisotropic properties of the medium give rise to stop bands where there is no propagation at all. The location and width of the bands depend on the material properties, more precisely on the degree of anelasticity and anisotropy. In contrast, they exist even for very weak anisotropy and very low-loss anelastic solids. A physical interpretation seems to be in order here. The bands correspond to nonphysical solutions since the phase velocity vanishes or is purely imaginary. A zero phase velocity corresponds to an infinite slowness, but the generation of a wave with such slowness is precluded. The same applies when the slowness takes an imaginary value. However, the effects of the bands should be observable near the threshold, that is when the value of the inhomogeneity angle is such that the phase velocity is small and the slowness is high along a given direction. Indeed, this is combined with a high attenuation that produces a substantial dissipation of the wavefield along the band directions, and this anomalous highly anisotropic attenuation is really an observable effect.

It is also remarkable that, contrary to the isotropic case, inhomogeneous body waves can propagate even for perpendicular propagation and attenuation directions. Numerical simulations in unbounded media confirm the validity of the theory in the framework of homogeneous viscoelastic plane waves. The discovery of the stop bands is likely to impact amplitude versus offset techniques (AVO) since, as with the Rayleigh window phenomenon, the bands can produce substantial variations in the recorded amplitudes. In fact, the existence of a stop band acting on inhomogeneous waves traveling between two interfaces will produce a variation in the reflected wavefield that might be confused with a variation in the reflectivity of the lower interface. Further work involves Snell's law for inhomogeneous waves in material interfaces separating dissipative anisotropic materials, the expressions for the reflection and transmission coefficients, and the investigation of the stop bands for qP and qSV waves. For this purpose, numerical modeling based on the full wave equation is essential to verify the theoretical assumptions.

ACKNOWLEDGMENTS

This work was supported in part by the Commission of European Communities under the GEOSCIENCE project.

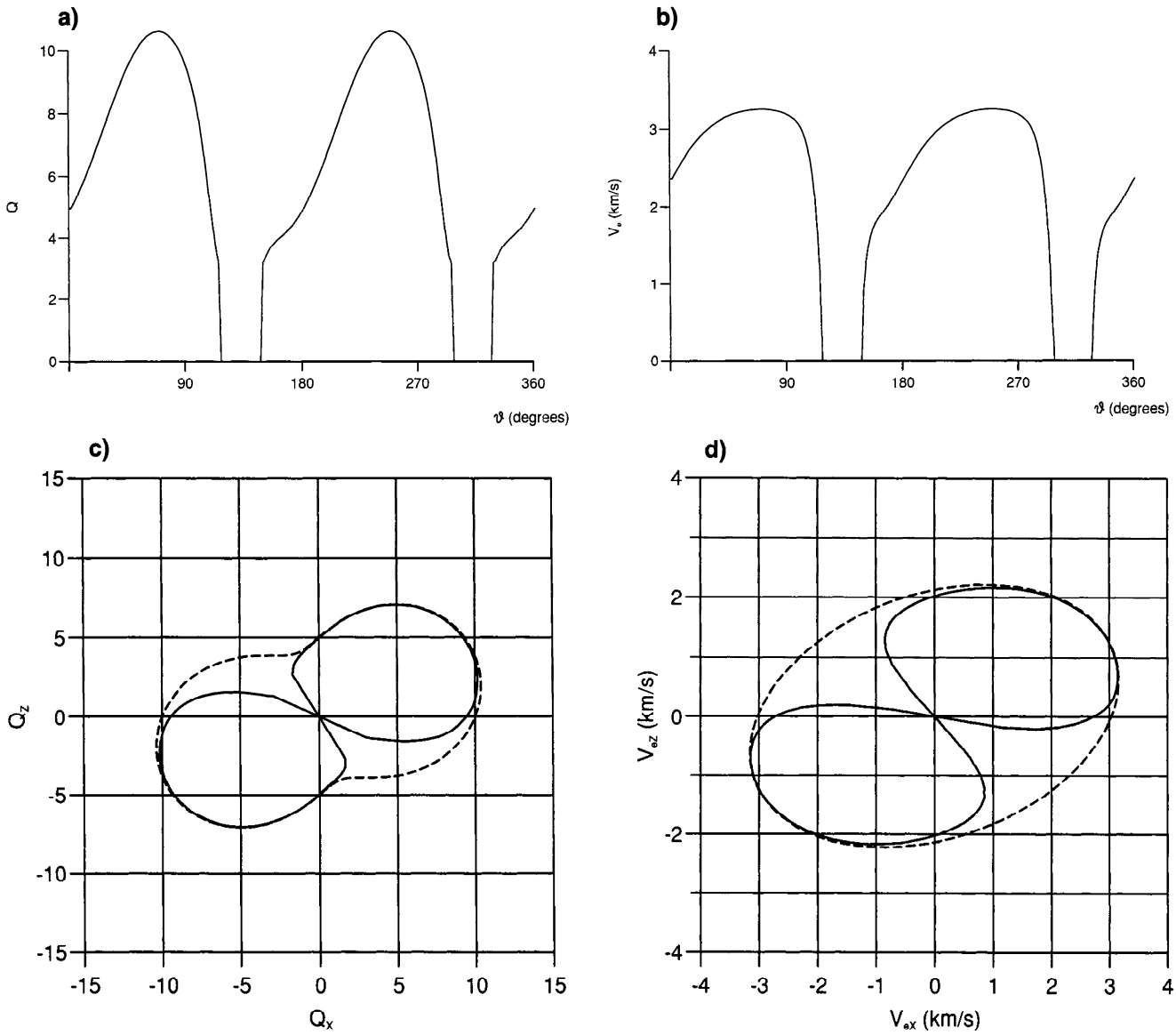

FIG. 4. Quality factor Q and energy velocity V_e are plotted versus propagation angle O-in Cartesian form-in (a) and (b), respectively. The corresponding polar plots are shown in (c) and (d). The material properties are those of Figure 3a, and the inhomogeneity angle is γ = 68 degrees.

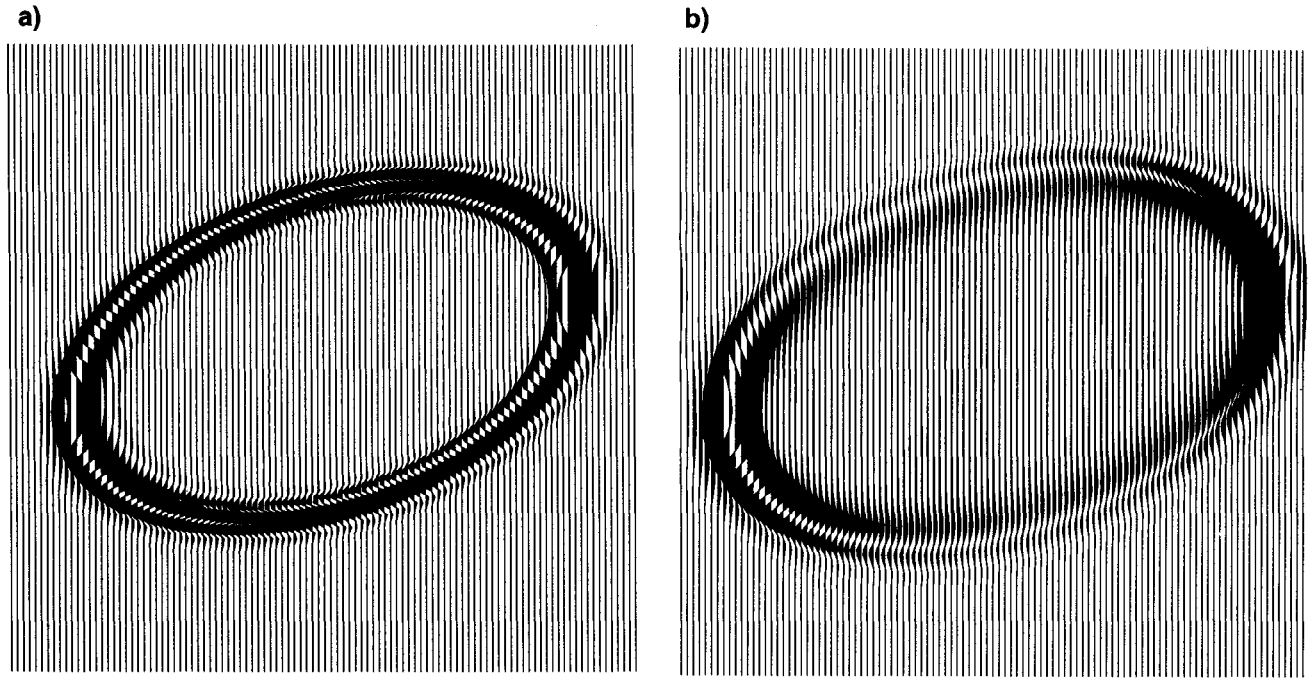

FIG. 3. Snapshots of (a) the elastic, and (b) the anelastic wavefields produced by a line source normal to the symmetry plane of a monoclinic medium. The source is a Ricker wavelet with central frequency of f_0 (Figure 2). The resulting wavefield is composed mostly of homogeneous waves.

REFERENCES

Auld, B. A., 1990, Acoustic fields and waves in solids, Vol. 1, second edition: Robert Krieger Publishing Co.

Borcherdt, R. D., 1977, Reflection and refraction of type-II S-waves in elastic and anelastic solids: Bull. Seis. Soc. Am., 67, 43-67.

Borcherdt, R. D., Glassmoyer, G., and Wennerberg, L., 1986, Influence of welded boundaries in anelastic media on energy flow, and characteristics of P, S-I, and S-II waves: Observational evidence of inhomogeneous body waves in low-loss solids: J. Geophys. Res., 91, 11503-11518.

Buchen, P. W., 1971, Plane waves in linear viscoelastic media: Geophys. J. Roy. Astr. Soc., 23, 531-542.

Carcione, J. M., 1990, Wave propagation in anisotropic linear viscoelastic media: theory and simulated wavefields: Geophys. J. Internat., 101, 739-750.

——— 1992a, Rayleigh waves in isotropic-viscoelastic media: Geophys. J. Internat., 108, 453-464.

- 1992b, Anisotropic Q and velocity dispersion of finely layered media: Geophys. Prosp., 40, 761-783.

- 1994, Wavefronts in dissipative anisotropic media, Geophysics, 59, 644-657.

Carcione, J. M., and Cavallini, F., 1993a, Energy balance and fundamental relations in anisotropic viscoelastic media: Wave Motion, 18, 11-20.

——— 1993b, Modeling anelastic shear waves in the symmetry plane of a monoclinic medium: SEG/CPS Beijing Internat. Geophys. Conference and Exposition, Expanded Abstracts, 448-449.

——— 1993c, Inhomogeneous pure shear waves in dissipative anisotropic media: 63rd Ann. Internat. Mtg., Soc. Expl. Geophys., Expanded Abstracts, 998-1001.

- 1993d, A semi-analytical solution for the propagation of pure shear waves in dissipative monoclinic media, Acoust. Lett., 17, 72-76.

Hosten, B., Deschamps, M., and Tittmann, B. R., 1987, Inhomogeneous wave generation and propagation in lossy anisotropic solids. Application to the characterization of viscoelastic composite materials: J. Acoust. Soc. Am., 82, 1763-1770.

Krebes, E. S., 1984, On the reflection and transmission of viscoelastic waves-Some numerical results: Geophysics, 49, 1374-1380.

Neumann, F. E., 1885, Vorlesungen uber die Theorie der Elastizitat, Leipzig.

Silva, M. A. G., 1992, Propagation of transverse anti-plane waves in orthotropic layers: Eur. J. Mech., A/Solids, 11, 849-862.

Winterstein, D. F., 1987, Vector attenuation: Some implications for plane waves in anelastic layered media: Geophysics, 52, 810-814.

APPENDIX A

UMOV-POYNTING VECTOR AND ENERGY DENSITIES FOR INHOMOGENEOUS SHEAR WAVES IN THE PLANE OF SYMMETRY OF A MONOCLINIC MEDIUM

The nonzero strain components associated with the anti-plane shear wave [equation (6)] are

$$S_4 = \frac{\partial u}{\partial z} = -\iota k_z U_0 e^{\iota(\omega t - \mathbf{k}\,\mathrm{l}\,\mathrm{x})}, \tag{A-1}$$

$$S_6 = \frac{\partial u}{\mathrm{ax}} = -\iota k_x U_0 e^{\iota(\omega t - \mathbf{k}\,\mathrm{l}\,\mathrm{x})}. \tag{A-2}$$

The nonzero stress components are, from equations (1) and (6),

$$T_4 = p_{44} S_4 + p_{46} S_6 = -\iota(p_{44} k_z + p_{46} k_x) U_0 e^{\iota(\omega t - \mathbf{k}\cdot\mathbf{x})}, \tag{A-3}$$

$$T_6 = p_{46} S_4 + p_{66} S_6 = -\iota(p_{46} k_z + p_{66} k_x) U_0 e^{\iota(\omega t - \mathbf{k}\cdot\mathbf{x})}.$$

(A-4)

From equation (23), the Umov-Poynting vector is

$$P = -\tfrac{1}{2}\dot{u}^*(T_4\hat{\mathbf{e}}_z + T_6\hat{\mathbf{e}}_x) = \tfrac{1}{2}\omega|U_0|^2 e^{-2\boldsymbol{\alpha}\cdot\mathbf{x}} \times [(p_{44}k_z + p_{46}k_x)\hat{\mathbf{e}}_z + (p_{46}k_z + p_{66}k_x)\hat{\mathbf{e}}_x]. \quad \text{(A-5)}$$

From equation (26), the average kinetic energy density is

$$\langle\varepsilon_v\rangle = \tfrac{1}{4}\rho\dot{\mathbf{u}}^{\top}\cdot\dot{\mathbf{u}}^* = \tfrac{1}{4}\rho\omega^2|U_0|^2 e^{-2\boldsymbol{\alpha}\cdot\mathbf{x}}. \quad \text{(A-6)}$$

From equation (25), the average potential energy density is

$$\langle\varepsilon_s\rangle = \tfrac{1}{4}\Re[p_{44}|S_4|^2 + p_{66}|S_6|^2 + p_{46}(S_4S_6^* + S_4^*S_6)], \quad \text{(A-7)}$$

which, after substitution of the strains (A-l) and (A-2), becomes

$$\langle\varepsilon_s\rangle = \tfrac{1}{4}|U_0|^2 e^{-2\boldsymbol{\alpha}\cdot\mathbf{x}}\Re[p_{44}|k_z|^2 + p_{66}|k_x|^2 + 2p_{46}\Re(k_xk_z^*)], \quad \text{(A-8)}$$

$$\langle\varepsilon_s\rangle = \tfrac{1}{4}|U_0|^2 e^{-2\boldsymbol{\alpha}\cdot\mathbf{x}}\kappa^2\Re\{p_{44}(\ell_z^2 + q^2m_z^2) + p_{66}(\ell_x^2 + q^2m_x^2) + 2p_{46}\Re[(\ell_x - \imath qm_x)(\ell_z + \imath qm_z)]\}, \quad \text{(A-9)}$$

where equations (8) and relation (15) have been used. Reordering terms, and using equations (11)-(13), the average strain energy density is

$$\langle\varepsilon_s\rangle = \tfrac{1}{4}\rho|U_0|^2 e^{-2\boldsymbol{\alpha}\cdot\mathbf{x}}\kappa^2\Re[a + q^2b]. \quad \text{(A-10)}$$

Similarly, the average dissipated energy density over a cycle is

$$\langle\varepsilon_d\rangle = \tfrac{1}{2}\rho|U_0|^2 e^{-2\boldsymbol{\alpha}\cdot\mathbf{x}}\kappa^2\Im[a + q^2b]. \quad \text{(A-11)}$$

APPENDIX B

PEAK STRAIN ENERGY DENSITY FOR HARMONIC FIELDS IN A GENERAL ANISOTROPIC MEDIUM

The strain energy density is given by

$$\varepsilon_s = \tfrac{1}{2}\Re[\mathbf{S}^{\top}]\,\Re[\mathbf{p}]\,\Re[\mathbf{S}]. \quad \text{(B-1)}$$

For a time harmonic field, the strain vector has the form

$$S = \mathbf{S}_0 e^{\imath\delta}, \qquad s = \omega t, \quad \text{(B-2)}$$

where $\mathbf{S}_0$ depends on the spatial coordinates. Then

$$\Re[\mathbf{S}] = \Re[\mathbf{S}_0]\cos S - \Im[\mathbf{S}_0]\sin\delta. \quad \text{(B-3)}$$

For clarity, we redefine

$$\mathbf{S}_\Re \equiv \Re[\mathbf{S}_0], \qquad \mathbf{S}_\Im \equiv \Im[\mathbf{S}_0], \qquad \mathbf{p}_\Re \equiv \Re[\mathbf{p}].$$

Substituting these expressions into equation (B-l), the strain energy takes the form

$$4\varepsilon_s = U + V\cos S - T\sin\delta, \quad \text{(B-4)}$$

where

$$U = \mathbf{S}_\Re^{\top}\cdot\mathbf{p}_\Re\cdot\mathbf{S}_\Re + \mathbf{S}_\Im^{\top}\cdot\mathbf{p}_\Re\cdot\mathbf{S}_\Im, \quad \text{(B-5)}$$

$$V = \mathbf{S}_\Re^{\top}\cdot\mathbf{p}_\Re\cdot\mathbf{S}_\Re - \mathbf{S}_\Im^{\top}\cdot\mathbf{p}_\Re\cdot\mathbf{S}_\Im, \quad \text{(B-6)}$$

$$T = \mathbf{S}_\Re^{\top}\cdot\mathbf{p}_\Re\cdot\mathbf{S}_\Im + \mathbf{S}_\Im^{\top}\cdot\mathbf{p}_\Re\cdot\mathbf{S}_\Re = 2\mathbf{S}_\Re^{\top}\cdot\mathbf{p}_\Re\cdot\mathbf{S}_\Im. \quad \text{(B-7)}$$

As can be seen by differentiating equation (B-4) with respect to t, the strain energy has a maximum at $\tan\delta_0 = -T/V$. Replacing this value into equation (B-4) gives

$$(\varepsilon_S)_{\text{peak}} = \tfrac{1}{4}(U + \sqrt{V^2 + T^2}). \quad \text{(B-8)}$$

Writing the strain as

$$\mathbf{S}_\Re = |S_K|\cos\phi_K\hat{\mathbf{e}}_K, \qquad \mathbf{S}_\Im = |S_K|\sin\phi_K\hat{\mathbf{e}}_K, \qquad K = 1, \ldots, 6, \quad \text{(B-9)}$$

implies that

$$U = |S_K||S_J|p_{KJ\Re}\cos(\phi_K - \phi_J), \quad \text{(B-10)}$$

$$V = |S_K||S_J|p_{KJ\Re}\cos(\phi_K + \phi_J), \quad \text{(B-11)}$$

$$T = |S_K||S_J|p_{KJ\Re}\sin(\phi_K + \phi_J). \quad \text{(B-12)}$$

The quantity U is four times the time average strain energy density [equation (25)]. In fact,

$$4\langle\varepsilon_s\rangle = \Re[\mathbf{S}^{\top}\,\mathbf{p}\cdot\mathbf{S}^*] = \Re[|S_K|e^{\imath\phi_K}p_{KJ}|S_J|e^{-\imath\phi_J}], \quad \text{(B-13)}$$

or

$$4\langle\varepsilon_s\rangle = |S_K||S_J|[p_{KJ\Re}\cos(\phi_K - \phi_J) - p_{KJ\Im}\sin(\phi_K - \phi_J)] = U, \quad \textit{(B-14)}$$

since the second term of the right-hand side vanishes (because of the symmetry of the stiffness matrix and the properties of the sine function). On the other hand,

$$V^2 + T^2 = |S_K||S_J||S_L||S_M|p_{KJ\Re}p_{LM\Re} \times \cos(\phi_K + \phi_J - \phi_L - \phi_M) \equiv 16\Delta^2. \quad \text{(B-15)}$$

Finally, the peak strain energy density for harmonic fields in a general anisotropic medium takes the form

$$(\varepsilon_S)_{\text{peak}} = \langle\varepsilon_s\rangle + A. \quad \text{(B-16)}$$

When all the strain components are in phase,

$$\Delta = \tfrac{1}{4}|S_K||S_J|p_{KJ\Re} = \langle\varepsilon_s\rangle, \quad \text{(B-17)}$$

and

$$(\varepsilon_S)_{\text{peak}} = 2\langle\varepsilon_s\rangle, \quad \text{(B-18)}$$

as is the case for homogeneous plane waves.